Plasma measurements with the TMX-U $E\|B$ end-loss ion spectrometers

J. H. Foote, B. E. Wood, M. D. Brown, and G. M. Curnow

Lawrence Livermore National Laboratory, University of California, Livermore, California 94550

(Presented on 10 March 1986)

Two $E\|B$ end-loss-ion spectrometers (ELIS) are now making plasma measurements on tandem mirror experiment-upgrade (TMX-U). One instrument is mounted on each end of this open-ended tandem-mirror machine. These spectrometers observe plasma losses along magnetic-field lines. They operate reliably and with a minimum of attention during an experimental run. Their data, which are quickly acquired and analyzed, help guide the experimental sequence. The parallel electric and magnetic fields separate the end-loss ions according to mass (D^+ and H^+) and energy. Each spectrometer detects ions with an array of 128 flat collector plates that are made from copper-coated G10 epoxy fiberglass, normally used for printed-circuit boards. The ELIS diagnostic system produces a wealth of experimental information, including data on peak plasma potential, central-cell ion temperature, potentials in the thermal-barrier region, axial confinement and ion-end-loss plugging, energetic-electron losses, and hydrogen/deuterium concentrations.

INTRODUCTION

Ions escape along magnetic-field lines out the ends of a tandem-mirror controlled-fusion experimental machine such as tandem mirror experiment-upgrade (TMX-U). These ions carry significant information about the confined plasma. To measure the energies and masses of these ions, we now have two end-loss-ion spectrometers (ELIS) mounted on TMX-U, one on each end.

These ELIS diagnostic instruments produce a wealth of experimental information. We are obtaining end-loss energy spectra much more detailed in energy and time than in previous measurements. With these data, we can determine key plasma parameters and characteristics such as peak plasma potential, thermal-barrier potential, central-cell ion temperature, axial confinement and ion-end-loss plugging, hydrogen/deuterium concentrations, magnetic-field location of potential peak, and energetic-electron losses.

Reference 1 is an earlier article on the ELIS, prepared during the construction of the first spectrometer. This article is a continuation of that work and includes experimental results obtained with our two spectrometers. References 2–5 contain additional information.

I. APPARATUS

The end-loss ions are analyzed with parallel magnetic and electric fields, which we usually set to detect deuterons (D^+) and protons (H^+). The electric field spatially separates the masses, and the magnetic field resolves the energy spectrum of each mass. Figure 1 shows this spatial separation. The greater the ion energy, the further the ion is displaced to the right of the entrance hole when it strikes the detector array.

An array of 128 flat collector plates measures the separated ions. Figure 2 shows the array with two rows of 60 detectors each—a row for the deuterons and a row for the protons. These 120 detectors are surrounded by eight border detectors to guard against ions missing the regular detectors. The spatial width of the 120 detectors is varied so that each covers the same energy range. The detector array is made of copper-coated G10 epoxy fiberglass, normally used for printed-circuit boards, with lines of copper etched away to make the individual detector plates.

The ions enter through the hole shown at the lower left of Fig. 2 and then curve around and move upward to reach the detectors. When properly centered vertically by the electric field, these ions reach the detectors in the region of the shaded bands. The numbers across the top represent the locations on the detector array of various deuteron and proton energies for one magnetic-field setting.

For further discussion of the experimental equipment, see Ref. 1.

II. EXPERIMENTAL RESULTS

Figure 3 shows the D^+ energy spectrum, measured five times per ms by one ELIS during an entire TMX-U plasma shot. The deuterium plasma initially forms at about 12 ms and terminates at about 75 ms. Each small tick mark at the bottom represents one detector of the upper row in Fig. 2. These results are typical of the detailed data we are obtaining on ion end loss (which originates principally in the central

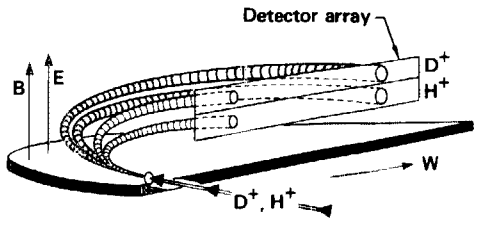

FIG. 1. Spatial separation of ions by mass and energy in the $E\|B$ region of the ELIS. The symbols E and B represent the electric and magnetic fields, respectively, and W is the ion energy. Shown are beamlets for two different D^+ and two different H^+ energies.

 0034-6748/86/081786-03$01.30

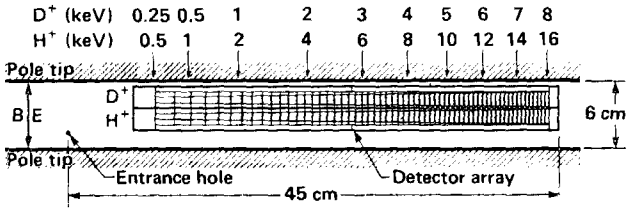

FIG. 2. The ELIS detector array of 128 flat collector plates that measures the separated ions.

cell) versus energy and time. From these results, we know that during a shot the energy spectrum can vary considerably in its shape and in its position on the energy scale. These variations can often be correlated with changes in experimental conditions.

We estimate the peak end-cell plasma potential and central-cell ion energy from measured energy spectra such as those shown in Fig. 3. We make a linear extrapolation to the baseline of the data on the low-energy side of an individual energy spectrum to estimate the peak potential. The rate of signal falloff on the high-energy side of the spectrum gives an estimate of the temperature of the central-cell ions.

Besides measuring the peak plasma potential in the end cell closest to it and the ion energy in the central cell, each ELIS can also sample the plasma potential in a region of the far end cell where we expect the tandem-mirror thermal barrier to be formed. To do this, we use a neutral beam injected at an angle (18 °) within the loss cone. This is indicated at the right of Fig. 4(a), which shows relative magnetic-field magnitude versus axial position throughout TMX-U. Because the injection angle is within the loss cone, any of the energetic beam atoms ionized by the plasma in the end cell at the right can travel through TMX-U and out the end at the left. These ions arrive in the vicinity of the electrically grounded ELIS [indicated schematically at the left of Fig. 4(b)] with energy equal to their original beam energy plus the energy corresponding to the plasma potential in the region where they were born.

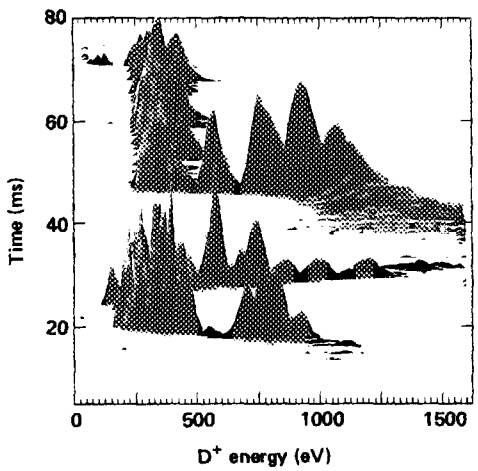

FIG. 3. Energy spectrum of end-loss D^+ during an entire TMX-U plasma shot, measured five times per ms.

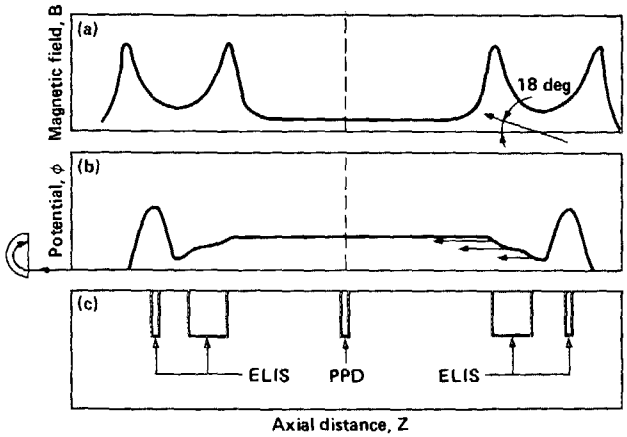

FIG. 4. Magnetic-field intensity and plasma-potential magnitude (with measuring locations) versus position along the magnetic axis: (a) schematic magnetic-field-intensity profile along the magnetic axis, showing injection angle and position of one neutral-beam potential probe; (b) possible thermal-barrier-type axial potential profile; and (c) axial regions over which we are now simultaneously measuring the plasma potential near the magnetic axis (with an ELIS and a neutral-beam potential probe at each end of TMX-U and the plasma potential diagnostic at the center).

Figure 4(b) shows a possible axial plasma-potential profile of the thermal-barrier type and also the approximate axial region over which ions can be produced by the neutral beam and, subsequently, detected by the ELIS. This axial region, indicated by the arrows at the right, is where the neutral beam intersects the bundle of magnetic-field lines observed by the ELIS. The higher the potential at which the ion is born, the more energetic the ion will be when it reaches the ELIS. This is denoted by the varying length of the arrows. The ions that are produced by the neutral beam and that reach the ELIS thus should have an energy spread and magnitude corresponding approximately to the range of potentials in the thermal-barrier region over which they are born. The neutral-beam potential probe is operated on hy-

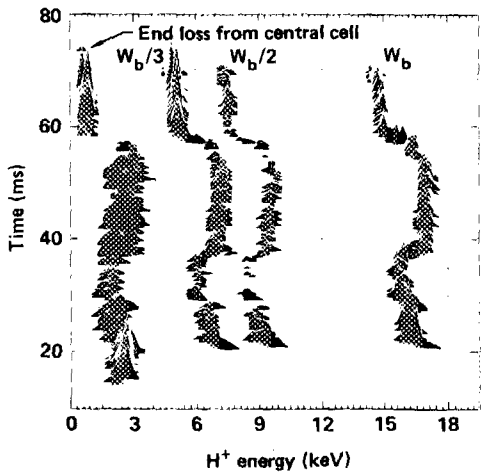

FIG. 5. Example of plasma-potential measurements using the three energy components of a neutral-beam probe. The quantity W_b is the full beam energy.

drogen gas so that the resulting ions are protons and, with our double row of detectors, are easily distinguishable from the deuterons emitted by our standard deuterium plasma.

The neutral beams normally have full-, half-, and third-energy components in them. The ELIS observes all three energy components, and each can provide information on the potentials in the thermal-barrier region at the opposite end cell.

Figure 5 is an example of plasma-potential measurements using the three energy components of a neutral-beam potential probe. At the end of this shot (top of plot), the plasma potential is very low, and the energies of the ions produced by the three neutral-beam components and detected by the ELIS are essentially the original energies of those neutral-beam components. Thus, the energy of the full-energy (W_b), half-energy ($W_b/2$), and third-energy ($W_b/3$) components are somewhat under 15, 7.5, and 5 keV, respectively. The low potential is confirmed by the low energy of the central-cell end losses. Earlier in this shot, near 50 ms, the measured energies of the three beam components are all over 2 keV higher than at the end of the shot. Thus, these ions were all born in a region of plasma potential greater than 2 keV, and they gained this added energy as they traveled to the grounded ELIS. The end-loss ions also have about 2 keV of energy, showing a similar potential in the end cell opposite to that in which the neutral-beam potential measurements were made.

In Fig. 4(c), we show the axial regions throughout TMX-U over which we are now simultaneously measuring the plasma potential near the magnetic axis. Besides data obtained with the ELIS instruments and neutral-beam potential probes on each end of the machine, measurements in the central cell with a heavy-ion-beam plasma-potential-diagnostic probe (PPD)[6] are also being made. We now have the ability to detect an axial plasma profile of the type drawn in Fig. 4(b).

III. CONCLUDING REMARKS

Our two end-loss-ion spectrometers provide useful and extensive data on plasma potentials and ion energies in TMX-U. They operate reliably and with a minimum of attention during an experimental run. Their data, which are quickly acquired and analyzed, help guide the experimental sequence.

ACKNOWLEDGMENT

This work was performed under the auspices of the U.S. DOE by the Lawrence Livermore National Laboratory under Contract No. W-7405-ENG-48.

[1]J. H. Foote, G. W. Coutts, L. R. Pedrotti, L. Schlander, and B. E. Wood, Rev. Sci. Instrum. **56**, 1117 (1985).
[2]B. E. Wood, J. H. Foote, G. W. Coutts, L. R. Pedrotti, and L. F. Schlander, in Proceedings of the 11th Symposium on Engineering Problems of Fusion Research, Austin, TX, 18–22 November 1985 (in press).
[3]J. H. Foote, Bull. Am. Phys. Soc. **30**, 1581 (1985).
[4]J. H. Foote, Bull. Am. Phys. Soc. **29**, 1390 (1984).
[5]J. H. Foote, D. P. Grubb, R. S. Hornady, and S. Falabella, Bull. Am. Phys. Soc. **28**, 1119 (1983).
[6]R. S. Hornady, D. Steele, and D. H. Nelson, Bull. Am. Phys. Soc. **30**, 1434 (1985).